

# Fabrication and empirical analysis of graphene dispersion/activated carbon on conductive networks in porous graphite felt supercapacitor

Brayden Noh

Auburn High School, 1701 E Samford Ave, Auburn, AL, United States

## ABSTRACT

Supercapacitors are a promising candidate for the regenerative braking system due to their inherent fast charging and high-current/temperature tolerance capabilities. However, most supercapacitors suffer from high weight to capacitance ratio, which averts the use of supercapacitors in regenerative braking in electric vehicles. This research proposes a new lightweight supercapacitor electrode fabrication, which consists of networking conductive layers of graphene dispersion and activated carbon in porous graphite felt using conductive ink. The composite electrode showed a specific capacitance up to  $170 \text{ F g}^{-1}$ , or  $13 \text{ F g}^{-1}$  from a completed device in type III deep eutectic solvent electrolyte, which gave the starting voltage of 2.3 V. The submersion fabrication alleviated the fabrication compare to brush method and production time was reduced to under 3 min of physical preparation.

## 1. Introduction

An increase in the use of electric propulsion in road vehicles in recent years has expanded interests in various methods to improve the efficiency for longer mileage and lower cost of the vehicle. This has opened for an opportunity for the regenerative braking system, which recovers partial kinetic energy to storable energy [1]. Supercapacitors, in its nature, has lower energy density and high-power density compare to a typical battery [2], which is why it is not found common as other power storing devices that need extensive charging. However, in electric vehicles, supercapacitors can be used to substitute batteries to provide their high-power during acceleration and regenerative braking. Batteries, on the other hand, can only provide a limited range of state-of-charge, which means providing their maximum charge in short pulses [3,4,5]. Current commercial supercapacitors usually suffer from high weight to capacitance ratio, since most applications are not required for weight constraints, such as grid power buffer and voltage stabilizer in electronics [6,7]. However, in electric vehicles, reducing the weight of the vehicle is crucial for longer mileage of the car [7], which has averted the use of supercapacitors in the regenerative braking system in current electric vehicle industry [8].

Porous carbons are currently used as an electrode material, with the most used being activated carbon due to its high surface area and low density [9,10,11]. However, the factor of capable capacitance is also influenced by pore structure and the conductivity of the electrode as the activated carbon itself has limited electrode performance due to the low conductivity and electrochemical kinetics [9, 12]. It has been shown in previous researches that the conductive network of graphene nanoplatelets in dispersions can help increase electrode conductivity and

increase pore accessibility, which has been shown to allow faster ion transportation and better access to activated carbon pores [13]. Also, researches show graphene nanoplatelet contained composite showed 23.5 times higher thermal conductivity than that of just powder AC [14].

The recent development of large-scale fabrication of graphene dispersion has made it possible to purchase graphene slurries at a lower cost [15, 16], which can be utilized in the electrode system to improve capacity. The knowledge of applications is still minimal as the material commercialization is relatively new. This research proposes a highly efficient and low-cost process in producing a supercapacitor using activated carbon and graphene dispersion. As electrolyte ion characteristics are mostly unknown in the supercapacitor electrode, this research aims to find the optimal ratios between activated carbon and graphene dispersion using empirical analysis.

## 2. Materials

Activated carbon (AC), graphene dispersion (GD), and graphite felt are employed for the composite synthesis. The AC in powder form is purchased from XFNano, and it shows a surface area at  $1800 \text{ m}^2/\text{g}$ . GD of 5–10  $\mu\text{m}$  lateral size is also purchased from the same supplier, and its main application was used as enhancing the thermal conductivity of composites. Fig. 1a and Fig. 1b show SEM images of the activated carbon. Fig. 1c and Fig. 1d show SEM image of the GD. Graphite felt is used as the conductive support for the electrode mixtures, and it was obtained from Zibo Ouzheng Carbon. Electrolyte consisted of choline chloride ( $\text{HOC}_2\text{H}_4\text{N}(\text{CH}_3)_3 + \text{Cl}^-$ ) (Acros > 99%) and ethylene glycol (Aldrich > 99%).

E-mail address: [swnoh@acsk12.org](mailto:swnoh@acsk12.org).

<https://doi.org/10.1016/j.est.2020.101264>

Received 3 January 2020; Received in revised form 30 January 2020; Accepted 31 January 2020

Available online 11 February 2020

2352-152X/© 2020 Elsevier Ltd. All rights reserved.

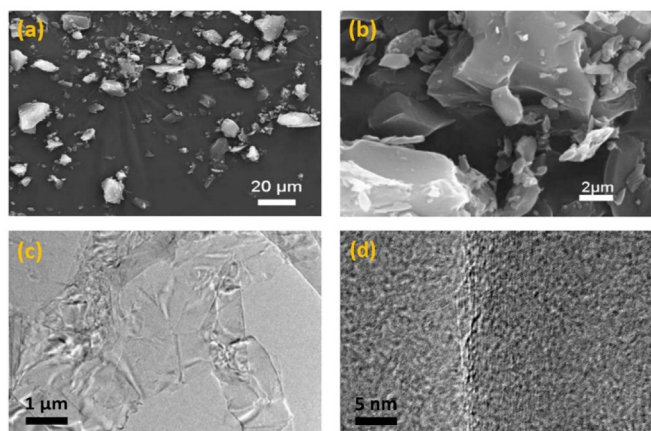


**Fig. 1.** (a) SEM image of the structural characterization of activated carbon at 20  $\mu\text{m}$  magnification, (b) SEM image of the structural characterization of activated carbon at 2  $\mu\text{m}$  magnification, (c) TEM image of graphene dispersion slurry at 1  $\mu\text{m}$  magnification, (d) HRTEM image of graphene dispersion slurry at 5 nm magnification.

### 3. Result

#### 3.1. Scalable fabrication of supercapacitor

The schematic of the entire process to form the supercapacitor, which was done with the perspective of scalable manufacturing process, is given in Fig. 2a. Fig. 2b shows the implementation of different materials in the electrode during the fabrication. During the initial process, graphite felt is submerged in conductive ink made from graphene dispersion and activated carbon, which was prepared in advance for faster process. The electrode composite was dried for 25 min before electrolyte coating on the top electrode surface. Activated carbon and

graphene dispersion are used to construct the conductive ink, which allows for high surface area and high conductivity.

#### 3.2. Electrode characteristics

Pre-fabrication electrode testing was conducted to find the best ratio for conductive ink fabrication, which is used to build the test supercapacitor on following stage. Electrode conductivity was measured using different weight ratios of AC to GD as shown in Fig. 3a. Because AC used in this research was semi-conductive, increasing AC weight decreased the conductivity of the electrode. GD and AC weight ratios of 1:8, 1:7, 1:6, and 1:5 showed high conductivity in the range of 3 to 6  $\text{Ohm}/\text{cm}^2$ . Surface area of 1 g of activated carbon provided 1800  $\text{m}^2/\text{g}$  based on the materials technical data sheet and electrode surface area was calculated based on the weight ratio of AC and GD in Fig. 3b. Balance the amount of the two materials impacts the capacity of the supercapacitor as the volume of conductive ink that is saturated in the graphite felt is bounded. Increase in the amount of AC allows for increase in ion pores and increase in the amount of GD allows for higher electrode conductivity. Due to the complexity of the factors that controlled the capacitance of the supercapacitor and the limited knowledge of the interaction between the new electrode and the DES solvent, empirical analysis was found to be most efficient. Total of 16 supercapacitors with different ratios of graphene dispersion and activated carbon were constructed to test the capacity of each electrode ratios. 36 electrodes sizing 1  $\text{cm}^2$  were prepared and the traditional painting fabrication was used to construct the supercapacitor as the method was proven to be easier in controlling weight variables of the materials. 1 ml of sodium sulfate aqueous electrolyte was coated on each of the electrode and low current of 20 mA was used to charge the supercapacitor for 30 s before testing the capacity. The usage of sodium sulfate electrolyte, instead of DES, and low current charging helped with stability and accuracy of the data [17], since it resulted in lower capacitance than normal testing condition. This specific fabrication method has been only used in finding the optimal electrode material ratios. After

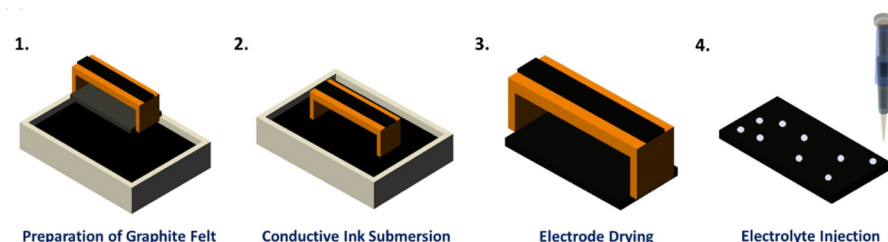
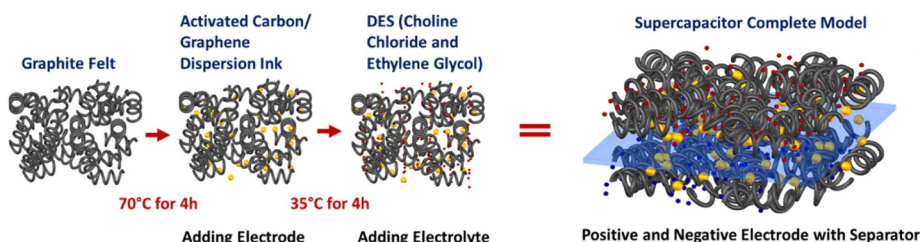


**Fig. 2.** (a) (1,2) Graphite felt is submerged in the ink for 5 s (3) Electrode composite is dried for 20 min at 60  $^{\circ}\text{C}$  (4) 10 ml of Electrolyte is Coated per 6  $\text{cm}^2$ . (b) Schematic illustration of composite electrode and electrolyte synthesis. Activated carbon and graphene dispersion ink are represented with yellow spheres and electrolyte is represented with red and blue spheres.

a: (1,2) Graphite felt is submerged in the ink for 5 seconds (3) Electrode composite is dried for 20 minutes at 60 $^{\circ}\text{C}$  (4) 10 ml of Electrolyte is Coated per 6  $\text{cm}^2$ .



b: Schematic illustration of composite electrode and electrolyte synthesis. Activated carbon and graphene dispersion ink are represented with yellow spheres and electrolyte is represented with red and blue spheres.

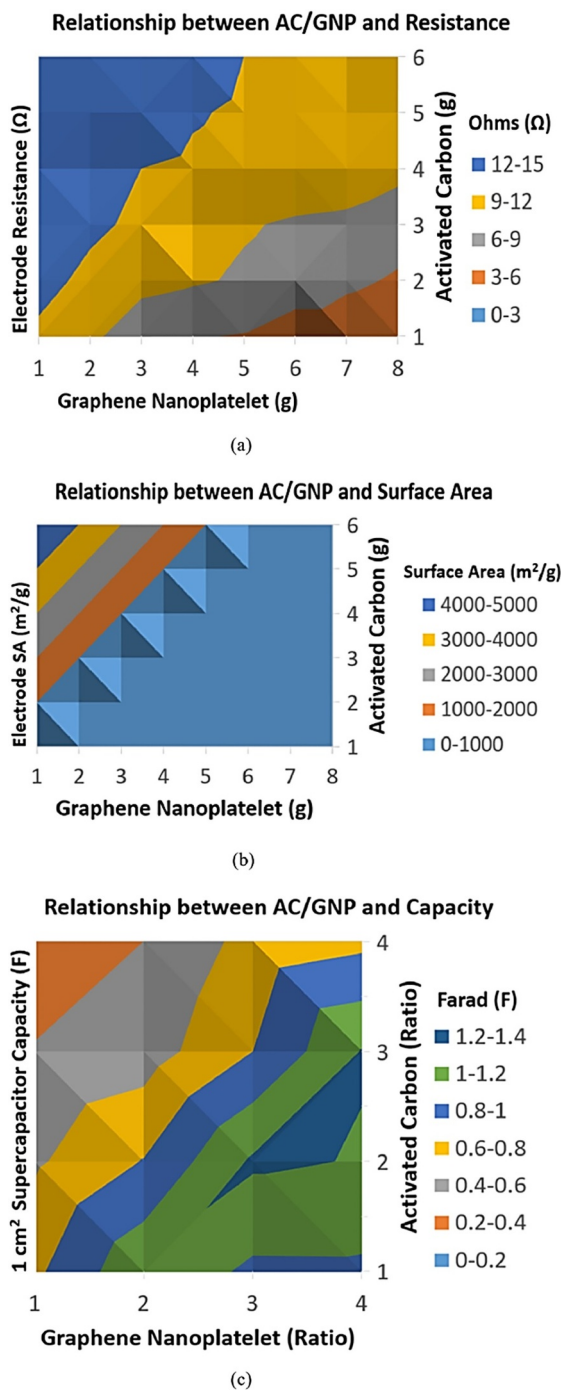


Fig. 3. (a) Outer shell electrode with different weight ratios of activated carbon and graphene dispersion's resistance is measured. (b) Surface area of the electrode based on the amount of electrode material is calculated using data numbers. (c) 1 cm<sup>2</sup> supercapacitors are built using different weight ratios of activated carbon and graphene to find the capacitance.

galvanic testing, electrodes with the ratio of GD to AC in range of 3:2.5 to 4:3 exhibited the highest capacity of 1.2 to 1.4 F cm<sup>-2</sup>, which can be seen from Fig. 3c. The range of these ratios was used to fabricate supercapacitors for capacitance measurement.

### 3.3. Supercapacitor capacitance

Supercapacitor's most important requirement is high capacitance and low weight ratio with capacitance. All the tests were performed

with galvanostatic charge and discharge technique, since data accuracy usually greater than cyclic voltammetry measurements. Current during charging was first measured to estimate the maximum charging rate and charging time through the research. All currents decrease as supercapacitor voltage value gets closer to the charging voltage. As seen in Fig. 4a, initial charging is very fast as current value loses half of its value at about 30 s of charging. After the 30 s mark, the current drop is much slower. Charging the supercapacitor over 10 V started bubbling of electrolyte and the current value did not decrease and no charge was shown during discharging. Fig. 4b shows the relationship between voltage and time when different current is applied. The specific capacitance was calculated using Eq. (1) [18].

$$Cs = I \cdot \Delta t / \Delta V \cdot m (Fg^{-1}) \quad (1)$$

Cs is the overall specific capacitance, I is the discharging current,  $\Delta t$  is the time in seconds it takes to discharge to certain voltage,  $\Delta V$  is the voltage difference, and m is mass of the supercapacitor. Overall specific capacitance is including weight of the entire supercapacitor including the Kapton tape insulation. This was measured instead of electrode weight specific capacitance, since overall specific capacitance gave more realistic idea of capacitance. The voltage curve constantly decreased, which confirm the EDLC characteristics of the samples. The supercapacitor mass was 2.5 gs, which showed the overall specific capacitance of 8.67 Fg<sup>-1</sup>, 7.46 Fg<sup>-1</sup>, and 5.68 Fg<sup>-1</sup> when 20 mA, 40 mA, and 60 mA were used to discharge respectively. The specific capacity decreased as discharge current increased, primarily due to the contribution of Ohmic drop. The current discharge test was also performed to 20 F commercial supercapacitor (8.5 g), which showed overall specific capacitance of 2.27 Fg<sup>-1</sup> when discharging at 20 mA, which meant the research supercapacitor showed about 4 times better specific capacitance in respect to the weight. With the perspective of supercapacitor usage in regenerative braking, repetitive charge-discharge testing was performed as can be seen in Fig. 4c and 4d. The two supercapacitors in two graphs were charged and discharged at same voltage and current. Fig. 4c was performed right after fabrication and Fig. 4d was performed 3 h after fabrication. Previous researches show that poor performance of supercapacitor is mainly caused by sluggish desolvation of ions at the pore opening and low ion migration within the pores. After 3 h, it was seen that supercapacitor sample's voltage increased slightly by 0.1 – 0.2 Vs, which led to increase in capacity of the supercapacitor. Fig. 4e shows low current discharge and coulombic efficiency rate, which was calculated with Eq. (1). Supercapacitor was seen to discharge at faster voltage values during the initial discharge phase (2.7 V to 1.2 V), which lasted for 200 s, but after 200 s, the voltage drop was significantly slower, with 0.65 V difference in the time range of 4000 s, which showed capacitance of 92.3 Farads or overall specific capacitance of 12.8 Fg<sup>-1</sup>, which was about 1.5 times better than capacitance when discharging at 20 mA. Coulombic efficiency was calculated using the Eq. (2) [18].

$$\eta = (t_d/t_c) \cdot 100\% \quad (2)$$

In this equation,  $t_d$  represents time for galvanic discharge and  $t_c$  represents time for galvanic charging. The efficiency was shown to be 96.30%, which shows high reversibility of electrode material for long term performance in supercapacitor. Also, the coulombic efficiency showed that the supercapacitor did not provoke additional chemical reactions, such as decomposition of the electrolyte, which degrades supercapacitor life. Fig. 4f shows the charge-discharge ratio during high voltage input. This was to simulate sudden high voltage input. Voltage range in the range of 5 V to 9 V were tested. It has been already acknowledged that high voltage damages the electrode. The purpose of this experiment was rather to see the supercapacitor's physical and chemical reaction than comparing capacitance at different charging voltage. Charging current value showed that above 9 V, the charging characteristic of current became abnormal, however Fig. 4f does show that supercapacitors at all tested charging voltage were able to



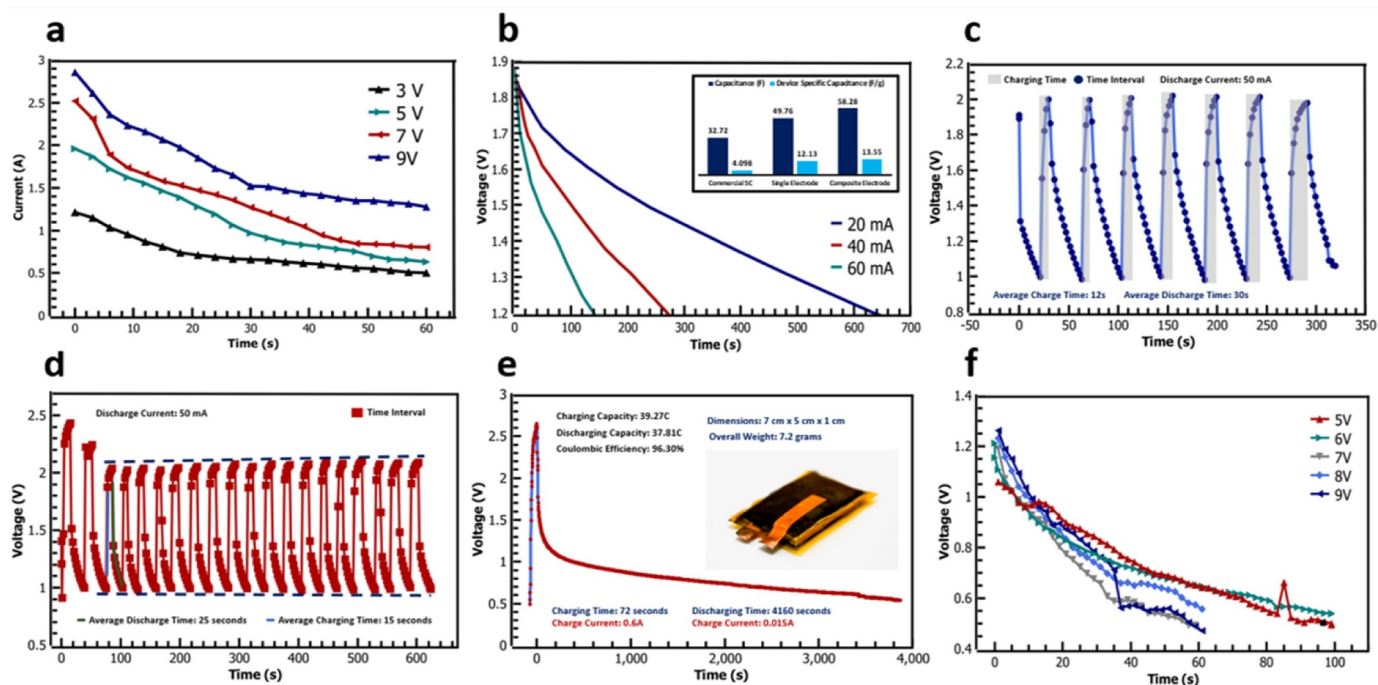


**Fig. 4.** (a) Charge-discharge comparison between commercial supercapacitor and this research supercapacitor, (b) Charge-discharge profile of the supercapacitor cell at different discharge current, (c) 10 cm<sup>2</sup> Electrode supercapacitor charge to discharge ratio when discharging at 50 mA and immediately after the fabrication, (d) Discharge characteristic from quick charge and high current 3 h after fabrication, (e) 15 g supercapacitor low discharge longevity testing, (f) Discharging characteristics at different overcharge voltages.

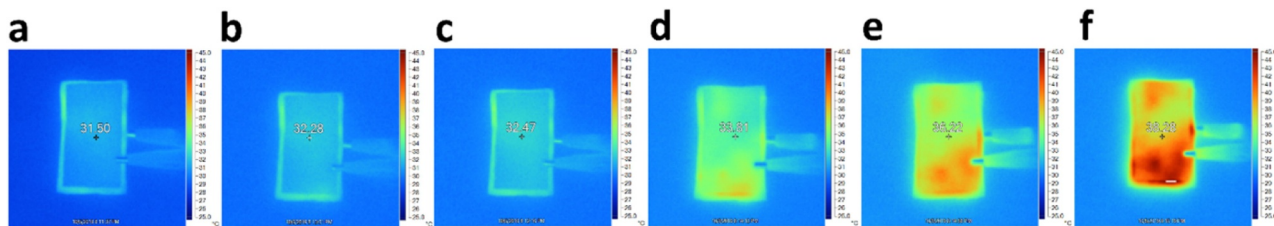


**Fig. 5.** Supercapacitor charging temperature measurement in different temperature after 30 s, (a) 2 V (b) 4 V (c) 6 V (d) 8 V (e) 10 V (f) 12 V.

discharge. Generally, as charging voltage increased, capacity decreased, which proves the physical damage of electrode due to heat. Charging to 5 V, 6 V, 7 V, 8 V, and 9 V showed capacitance of 6.24 F, 6.13 F, 5.31 F, 5.2 F, and 5.16 F respectively. Electrolyte breakdowns was tested with temperature sensor and bubbling voltage rates, which were performed simultaneously. Fully assembled supercapacitors were charged at different voltages, starting from 2 V and incrementing 2 V until 12 V, which was the maximum allowed voltage during the experiment condition. The electrode size was 3 cm<sup>3</sup>. Shown in Fig. 5, charging at 2 V, 4 V, and 6 V, did not show significant temperature change and the average temperature in respect to charging voltages were 31.5 °C, 32.28 °C, and 32.47 °C. Starting at 8 V, electrode temperature increased to 33.81 °C, 10 V resulted in 36.22 °C, and 12 V resulted in 38.28 °C. This experiment showed that charging the sample supercapacitors above 6 V was possible but led to faster degradation of the supercapacitor.

#### 4. Conclusion

Optimizing high-surface area activated carbon and graphene nanoplatelet mixture to create supercapacitor resulted in 4 times higher capacitance compares to commercial supercapacitors in similar mass. The supercapacitor was constructed with the perspective of lower-cost materials and fast manufacturing abilities. By using this novel

composite electrode and type III deep eutectic solvent, the developed supercapacitor not only exhibits high capacity and physically lightweight, but also possesses repeatability with excellent columbic efficiency that is comparable to commercial supercapacitors.

#### 5. Method

As the first stage of the supercapacitor fabrication, the conductive ink is prepared. 35 g of 5 wt.% GD is sonicated in 20 kHz for 15 min. 30 g of AC is then added to the dispersion, and the mixture is moved to magnetic stirrer for 2 min at 300 RPM. The graphite felt is than submerge in the aqueous mixture until all the felt pores are saturated. As a reference, a 3 cm<sup>3</sup> graphite felt soaked up 7 ml of conductive ink. To minimize leaking of the ink, the felt is held in the air for 5 min, giving the outer layer of the conductive ink dry. The electrode is then rested for heated 60 °C for 20 min. The remaining conductive ink can be used several times for the fabrication. The deep eutectic mixture was prepared, as reported by previous studies [19,20]. In the electrolyte used in this supercapacitor research, 8.5 g choline chloride and 30 ml ethylene glycol were added and stirred and heated to 70 °C until a homogeneous and clear liquid is formed. Fabrication of the electrode composite is completed after 10 ml of electrolyte is coated on both electrodes and rested for 3 h for the distribution of electrolyte ions in the electrode composite.

## Author contribution

I have conceived the idea and directed all the work. I have researched and purchased all the materials used in the research, experimented and fabricated the supercapacitor, tested the supercapacitors, and wrote the manuscript.

## References

- [1] A. Sakai, T. Miyazaki, T. Okano, K. Nimura, D. Nakata, Regenerative braking systems, *Encyclopedia Automotive Eng.* (2014) 1–15.
- [2] B.E. Conway, *Electrochemical Supercapacitors, Scientific Fundamentals and Technological Applications*, Kluwer, New York, 1999.
- [3] A. Jossen, Impact of dynamic driving loads and regenerative braking on the aging of lithium-ion batteries in electric vehicles, *J. Electrochem. Soc.* (2017) 3081–3085.
- [4] A. Burke, H. Zhao, Applications of supercapacitors in electric and hybrid vehicles, ITS UC Davis (2015).
- [5] P. Keil, Aging of lithium-ion batteries in electric vehicles: impact of regenerative braking, *Kintex* (2015) 2–4.
- [6] H. Liu, C. Mao, J. Lu, D. Wang, Electronic power transformer with supercapacitors storage energy system, *Electric Power Syst. Res.* 79 (8) (2009) 1200–1208.
- [7] Y.S. Wong, C.C. Chan, Vehicle energy storage vehicle energy storage, batteries vehicle energy storage batteries, *Transport. Technol. Sustain.* (2013) 1082–1102.
- [8] F.J. Perez-Pinal, C. Nunez, R. Alvarez, I. Cervantes, Power management strategies for a fuel cell/supercapacitor electric vehicle, 2007 IEEE Vehicle Power and Propulsion Conference, 2007.
- [9] E. Frackowiak, F. Beguin, Carbon materials for the electrochemical storage of energy in capacitors, *Carbon N Y* 39 (2001) 937.
- [10] G. Wang, L. Zhang, Zhang J, A review of electrode materials for electrochemical supercapacitors, *Chem. Soc. Rev.* 41 (2012) 797–828.
- [11] F. Beguin, V. Presser, A. Balducci, E. Frackowiak, E. Supercapacitors, carbons and electrolytes for advanced supercapacitors, *Adv Mater* 26 (2014) 2283.
- [12] A.C. Rodrigues, E.L.D. Silva, S.F. Quirino, A. Cuña, J.S. Marcuzzo, J.T. Matsushima, et al., Ag@Activated carbon felt composite as electrode for supercapacitors and a study of three different aqueous electrolytes, *Materials Res.* (2018).
- [13] Y. Qing, Boosting the supercapacitor performance of activated carbon by constructing overall conductive networks using graphene quantum dots, *J. Materials Chem. A* (2019).
- [14] A. Pal, K. Uddin, K.A. Rocky, K. Thu, B.B. Saha, CO<sub>2</sub> adsorption onto activated carbon–graphene composite for cooling applications, *Int. J. Refrigeration* 106 (2019).
- [15] A. Liang, Recent development concerning the dispersion methods and mechanisms of graphene, *Coatings MDPI* (2018) 12–17.
- [16] S. Shin, D. Bae, The effect of mechanically exfoliated graphene dispersion on the mechanical properties of aluminum/graphene composites, *Light Metals 2014* (2014) 1441–1442.
- [17] C. Zhong, A review of electrolyte materials and compositions for electrochemical supercapacitors, *Chem. Soc. Rev.* (2015) 7488–7491.
- [18] N. Zaki, A symmetric supercapacitor based on 30% poly (methyl methacrylate) grafted natural rubber (MG30) polymer and activated carbon electrodes, AIP Conference Proceedings, 2017.
- [19] L. Milla, Bio-inspired choline chloride-based deep eutectic solvents as electrolytes for lithium-ion batteries, *Elsevier Solid State Ionics* (2018) 44–48.
- [20] A.P. Abbott, D. Boothby, G. Capper, D.L. Davies, R.K. Rasheed, Deep eutectic solvents formed between choline chloride and carboxylic acids: versatile alternatives to ionic liquids, *J. Am. Chem. Soc.* 126 (29) (2004) 9142–9147.

I, Sangwon (Brayden) Noh, certify that they have NO affiliations with or involvement in any organization or entity with any financial interest (such as honoraria; educational grants; participation in speakers' bureaus; membership, employment, consultancies, stock ownership, or other equity interest; and expert testimony or patent-licensing arrangements), or non-financial interest (such as personal or professional relationships, affiliations, knowledge or beliefs) in the subject matter or materials discussed in this manuscript.